

Magnetoresistance of mesoscopic granular ferromagnets

A. Y. Dokov, H. Vilchik, and A. Frydman

The Minerva Center, The Department of Physics, Bar Ilan University, Ramat Gan 52900, Israel
(Dated: April 14, 2024)

We have performed magnetoresistance (MR) measurements of granular ferromagnets having lateral dimensions smaller than 0.5 μm and containing a small number of grains (down to about 100). Compared to macroscopic samples, these granular samples exhibit unusually large saturation fields and MR amplitudes. In addition, the evolution of the magnetoresistance curve as the intergrain distance decreases is qualitatively different than that of large samples. We discuss these results and suggest that they reflect a transition from percolation to quasi single-channel dominated transport.

PACS numbers: 73.23.-b; 73.40.Rw; 75.50.Cc

I. INTRODUCTION

Insulating granular ferromagnets, i.e. systems of magnetic grains imbedded in a non-magnetic insulating matrix, exhibit negative magnetoresistance (MR) curves. At zero magnetic field ($H = 0$) the resistance is maximal. For applied H the resistance decreases until, for large enough field, it reaches saturation. This behavior was observed in a variety of granular samples [1, 2, 3, 4, 5, 6, 7] and has been ascribed to spin dependent tunneling between randomly oriented magnetic moments of the grains [8, 9]. Applying a magnetic field aligns these moments, causing the tunneling resistance to decrease. The magnetoresistance is thus determined by the relative magnetic orientation of pairs of grains. The MR amplitude (defined as $R = R = \frac{R(H=1) - R(0)}{R(0)}$) of a pair of grains i and j is given by [10]:

$$\frac{R}{R} = \frac{1 + P^2 \cos(\theta)}{1 + P^2} - 1 \quad (1)$$

where P is the electron polarization and θ is the angle between the moment orientations at zero magnetic field. In the presence of magnetic field, H , the magnetic orientation of each grain is governed by two factors. The first is the magnetization easy axis of the grain due to its anisotropy, and the second is the external magnetic field. The total magnetic energy of a grain per unit volume is given by [11]:

$$\frac{W}{V} = \frac{\mu_0}{2} M_s^2 \sin^2(\theta) - \mu_0 M_s H \cos(\theta) \quad (2)$$

where μ_0 is magnetic permeability in vacuum, θ is the anisotropy coefficient (of the order of 1), M_s is the saturation magnetization, θ is the angle between the magnetic moment orientation and the easy axis of magnetization and ϕ is the angle between the magnetic moment and the applied magnetic field. Eq. 2 is composed of two energies. The left component, W_I , represents the energy due to orientation out of the easy axis and the right component, W_H is due to alignment of the moment with an

external field. The magnetic orientation of each grain (and therefore the MR amplitude) at zero temperature is determined by minimizing the energy of equation 2. It should be noted that ultrasmall grains at finite temperatures undergo a superparamagnetic transition, thus the thermal energy, $k_B T$, may dominate and overcome the effect of the magnetic energy.

When dealing with transport properties through a granular insulator, one has to take into account that not all the grains participate in the conductance processes since it is a strongly disordered system. It has long been realized that a percolation treatment is the proper way to deal with such a system as it provides much insight into the physics of the conductivity [12, 13, 14]. In this approach each pair of grains i and j is represented by a resistor with resistance R_{ij} inversely proportional to the hopping probability between the grains and given by [15]:

$$R_{ij} = R_0 \exp\left[\frac{2r_{ij}}{\lambda} + \frac{E_{ij}}{k_B T}\right] \quad (3)$$

where r_{ij} is the distance between the grains, λ is the localization length representing the decay of the electronic wavefunction in the insulator and E_{ij} is the energy difference between the electronic states. For metallic grains at temperatures of the order of a few K, E_{ij} is related to the charging energies of the grains which depend on the grain diameters. In general, smaller grains give rise to larger E_{ij} s. The granular system can be mapped by a resistor network containing series and parallel current paths. Because the network contains a wide distribution of resistances (due to the exponential factors in Eq. 3) the transport is percolative and governed by a set of critical resistors. These act as "red bonds" of the percolation network and their conductivity determines the transport properties of the entire system. Hence, the scale of inhomogeneity is the percolation radius, L_C , which can be viewed as the average distance between critical resistors.

As the lateral dimension of the sample is reduced below L_C , the nature of the transport is expected to change dramatically. A percolation network is no longer a suitable way to treat the system. Instead, a single current path, or even a single critical resistor, is expected to dom-

inate the transport, giving rise to mesoscopic effects and large sample to sample fluctuations.

In this paper we study the MR curves of granular ferromagnets with sizes smaller than L_C ($\sim 0.5 \mu\text{m}$) and compare them to the properties of macroscopic samples. We find that reducing the size causes a dramatic increase in both MR amplitudes and saturation fields. In addition, the evolution of the MR curve as a function of average inter-grain separation is different than that of large samples. We discuss these results and attribute them to a crossover from percolation transport to a single dominating current trajectory, as the sample size is reduced below the percolation radius.

I. EXPERIMENTAL

The samples described in this paper were discontinuous Ni films prepared by "quench condensation" [16, 17, 18, 19], i.e. evaporation of thin, discontinuous films on substrates that are kept at cold temperatures and under UHV conditions as described elsewhere [6, 7]. This technique enables one to perform electric and magnetic measurements during the sample growth. Thus, one can study the magneto-transport properties of a single granular Ni sample as a function of film thickness. We note that the thickness barely changes during the experiment. Adding $\sim 1 \text{ \AA}$ to a film of nominal thickness 30 \AA is sufficient to reduce the sample resistance by a few orders of magnitude [7]. This demonstrates that the decrease in resistance occurs due to increasing of inter-grain coupling while the grain sizes remain practically constant during the sample growth process. Thus the quench condensation method enables one to study the magneto-transport of granular ferromagnets as a function of the mean inter-grain distance without thermally cycling the sample or exposing it to atmospheric conditions.

In order to study small sized granular samples we combined photo-lithography and atomic force microscope (AFM) fabrication methods with quench-condensation. First we prepared Ni wires having width of a few μm on a SiO_2 substrate by conventional lithography. Next we used an AFM tip (with the z feedback loop disabled) to cut the wire in two, thus creating two close electrodes. The nano-space formed between the electrodes defined the geometry of the measured sample. The properties of the nano-space were determined by the quality of the AFM's tip, the force that was applied on the wire and the smoothness of the Ni. A typical electrode configuration is shown in the inset of Fig. 1. Once a desired geometry was achieved, the substrate was placed on a quench-condensation probe and a granular film was evaporated into the gap. Using this technique we were able to prepare samples with sizes as small as a few tens of nm. Since the grain diameters are of the order of 10-15 nm [20, 21] these samples contain about 100 grains. We name all samples with lateral dimensions smaller than

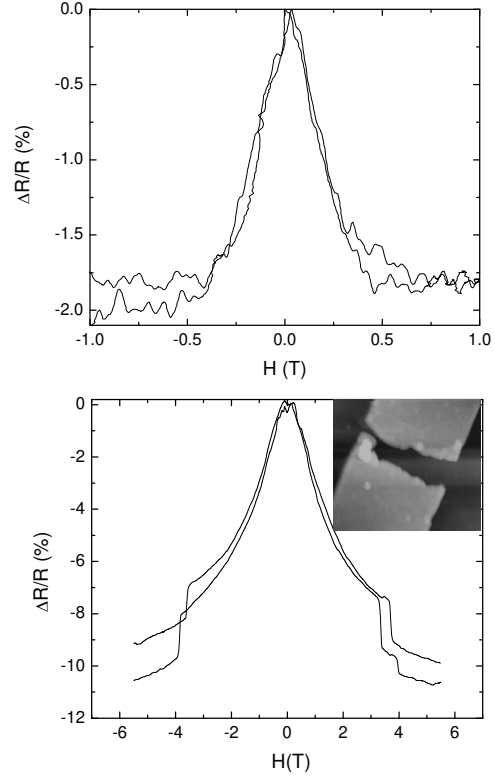


FIG. 1: $R=R$ for a $3\mu\text{m} \times 3\mu\text{m}$ sample (top panel) and a $100\text{nm} \times 100\text{nm}$ sample (bottom panel). The inset is an AFM image of the mesoscopic electrode template. A gap with lateral dimensions of 100nm is cut from a Ni wire having width of $3 \mu\text{m}$.

$0.5 \mu\text{m}$ "mesoscopic samples", while larger samples are named "macroscopic samples"

I. RESULTS

Magnetoresistance (MR) curves of two samples, one macroscopic and one mesoscopic, having sheet resistance of $2 \text{ M}\Omega$ (nominal thickness of 21 \AA), are depicted in Fig. 1. The magnetic field in these experiments was applied perpendicular to the film plane. The MR amplitude of the macroscopic sample is 2% and the saturation field, H_S , is $\sim 0.5 \text{ T}$. These values are typical of all our macroscopic 2D granular samples and are similar to those obtained by other groups using different preparation methods for fabrication of insulating granular ferromagnets [1, 2, 3, 4, 5]. A saturation field of 0.5 T can indeed be expected since it is close to $H = 4 M_S$, M_S being the saturation magnetization, which is the field required to align a thin Ni film perpendicular to the substrate against the shape anisotropy.

Unlike macroscopic samples, the mesoscopic samples exhibited large sample to sample variations of both MR amplitudes and saturation fields. H_S is always larger

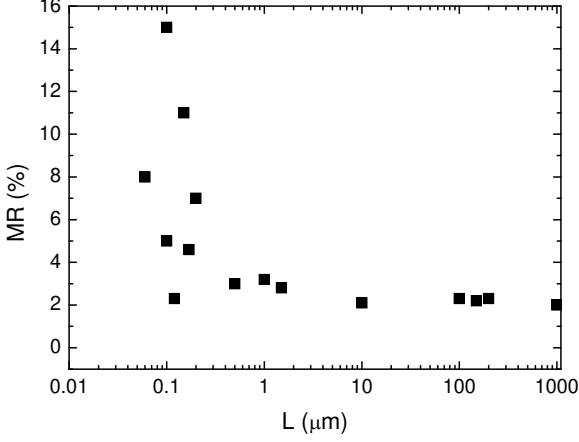


FIG. 2: $R=R$ for different samples having sheet resistance of $2M\Omega$ as a function of sample lateral size

than the typical value of $0.5T$ and varies between $1T$ to fields higher than $6T$ (the largest available field). $R=R$ also fluctuates substantially from sample to sample, however, the average MR amplitude sharply increases with decreasing sample size as seen in Fig. 2.

As material is added to the sample and the sheet resistance, R , decreases, several trends are observed in the macroscopic samples [6, 7]. The saturation field, H_s , remains constant at a value of $0.5T$ throughout the entire sample growth process (Fig. 3c). The MR amplitude, on the other hand, decreases monotonically and smoothly, until, for $R < 0.5k\Omega$, it is suppressed altogether (Fig. 3a). This can be expected since adding material causes coalescence of grains. For thick enough layers the sample is simply a continuous Ni film in which no spin dependent tunneling resistance is expected.

Another observed trend is the splitting of the MR peak. For high resistance the MR curve is centered at $H = 0$ as seen in Fig. 1. Upon decreasing resistance, the curve splits into two peaks and a hysteresis develops in the MR curve [6, 7]. The coercivity, H_c , grows as a function of decreasing R and reaches $0.25T$ for the lowest resistance in which MR is measurable (Fig. 3b). This was attributed to the increase of the effective grain size as the resistance decreases, thus giving rise to a transition from a non-hysteretic superparamagnetic sample to a ferromagnetic sample [6].

The mesoscopic samples show qualitatively different results. The MR amplitude does not decrease throughout most of the sample growth process. On the contrary,

$R=R$ appears to increase initially as material is added to the sample (Fig. 3a). Only for resistances smaller than $50k\Omega$ a sharp decrease in the magnetoresistance is observed. A similar effect is seen for the saturation field, H_s . It remains constant for most of the growth and decreases sharply (apparently approaching the bulk value

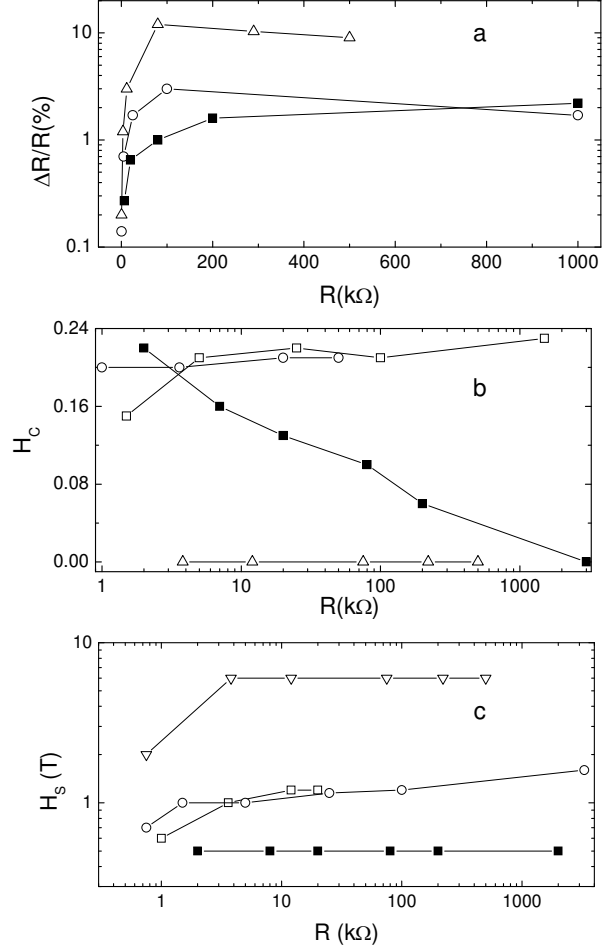


FIG. 3: The evolution of $R=R$ (top panel), the coercivity H_c (middle panel), and the saturation field H_s (bottom panel), as a function of resistance obtained as material is added to the sample. Full squares are for a macroscopic sample and open symbols are for a number of mesoscopic samples.

of $H = 4 M_s$ ($0.5T$) when the resistance drops below a few $k\Omega$ as seen in Fig. 3c.

Mesoscopic samples differ from macroscopic ones in the evolution of H_c as well. The mesoscopic systems show no development of hysteresis as a function of resistance. Some of our samples have no hysteresis for the initial deposition stages, and no hysteresis is observed even for the lowest measured resistance. Other samples exhibit a two peak MR curve even for the initial evaporation stages. In these samples the initial coercivity does not increase as material is added to the system (see Fig. 3b).

I. DISCUSSION

In order to understand these results we note that our mesoscopic systems are smaller than the percolation ra-

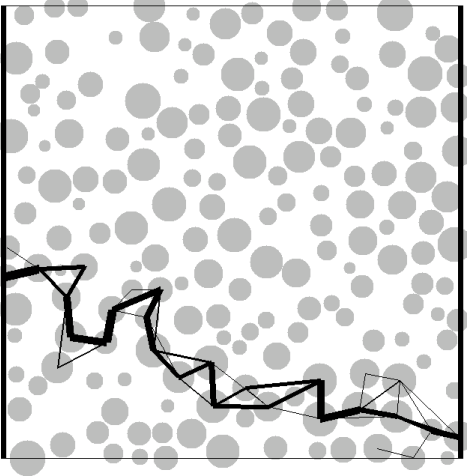


FIG. 4: Simulation of the current trajectories in a mesoscopic sample containing 180 grains, showing a single dominating current trajectory. Two leads are connected to the sample on the left and right edges, with a small d.c. voltage applied between them. The line width is proportional to the current flow magnitude.

dus, L_C . We have performed computer simulations of the MR of our granular Ni containing a small number of grains [22]. For systems with less than about 500 grains we find that the transport is governed by a single dominating channel. The current trajectories branch out, forming a complex percolating network, only for larger samples. This corresponds to L_C of about 25 grains across, which, in our samples, is equivalent to a sample size of about $0.5 \mu\text{m}$. For smaller samples the current is forced to flow through a single dominating chain of grains (see Fig. 4). The mesoscopic nature of these sample accounts for the large sample to sample variations of the MR curves in the small samples. We suggest that our results can be understood if we assume that the same chain of grains dominates the transport throughout the sample growth, from a configuration of electrically isolated grains until the sample is close to the metallic state. Adding material does not significantly alter this current path. The resistance decreases because the inter-grain distance is reduced but the MR amplitude does not reduce until the grains coalesce, the film becomes continuous and tunnelling MR is no longer expected. This is very different to the situation in large samples in which adding material opens up new channels and modifies the percolation network.

One consequence of the above model is that the electric current in small samples may flow through relatively small grains. In macroscopic samples, hopping through very small grains is energetically unfavorable due to a large contribution to E_{ij} in Eq. 3. The current can bypass very small grains and choose larger grains to con-

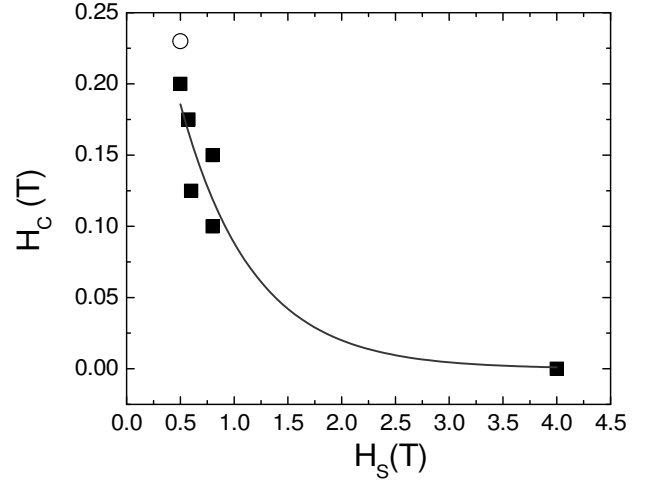


FIG. 5: The coercive field, H_C , determined from the field position of the MR peak, as a function of the saturation field, H_S , for different small samples (solid squares) and a large sample (empty circle). The solid line is a guide to the eye.

struct the transport network. This was shown in reference [7] where the coercivity extracted from MR measurements was found to be larger than that extracted from magnetization measurements demonstrating that the percolation network is constructed of grains larger than the average. In small samples the situation is different since the transport may be forced to take place through smaller grains. The fact that only few grains are present between the electrodes forces the conducting electrons to hop to small grains with large charging energy. This may explain the large saturation fields observed in our mesoscopic samples. The magnetization of grains having diameters smaller than 10 nm was shown to consist of ferromagnetically aligned core spins and a spin-glass-like surface layer [23]. Canting of the surface spins introduces magnetic stiffness of the grain moment since aligning them requires an extremely large external magnetic field. Another reason for large H_S in small grains is the effect of thermal fluctuations on the magnetic moment orientation. As shown in Eq. 2, the magnetic energy is proportional to the grain volume. For small, superparamagnetic grains, the energy due to the external H , W_H , has to overcome the thermal energy rather than the energy due to the easy axis, W_I . Therefore, the smaller the particle the larger the effects of surface moments and temperature, giving rise to large H_S . As the granular sample size is reduced, the average grain size participating in the transport decreases. This may account for the large saturation fields in our mesoscopic samples. Indeed, we observe a clear correlation between large saturation fields and small hysteresis in the MR curve (see Fig. 5) reflecting the role played by small grains in causing large H_S .

The behavior of the H_C can also be interpreted apply-

ing the above considerations. The crossover from non-hysteretic to hysteretic MR curves in large samples is attributed to an increase in the average grain size in the current network. Adding material to a granular array causes clustering of the transport network, adding parallel trajectories which allow the current to flow through larger grains. H_C thus increases as the resistance of the sample is decreased. In mesoscopic samples this process does not occur since the current path is relatively fixed throughout the sample growth process. Hence, the grains that participate in the transport for high R are expected to dominate at low R as well (though the inter-grain tunneling rate is larger). This accounts for the constant H_C observed in the mesoscopic samples.

A more subtle issue is that of the MR magnitude. The average MR of a random array of N grains (according to Eq. 1) is expected to be $(\frac{1}{1+p^2} - 1)$. Our simulations [22] show that for our Ni films this should produce an average $R=R$ value of about 10% [24]. Our macroscopic samples exhibit significantly smaller values. In addition, Fig. 2 shows that the smaller the sample the larger is the average MR value. The reason for this is not clear. Naively, one could expect that a denser network would emphasize the importance of trajectories with small mis-match of magnetic moment orientation. Our simulations show, however, that the average MR amplitude does not depend on the number of parallel channels. This discrepancy between experiments and theory impels us to suggest that the MR in the granular ferromagnets is affected by magneto-static dipole-dipole interactions which cause alignment of the magnetic moments of the grains even in the absence of magnetic field. Indeed, we have observed signs for magnetic interactions in different granular Ni systems [21]. If ferromagnetic correlations are significant in the granular sample, they may lead to a reduction of the measured $R=R$ relative to the theoretical expectations. In this case Eq. 2, representing the total magnetic energy of a grain, i , should contain an additional factor due to magnetic interaction with a neighbor grain, j :

$$\frac{W_{GG}}{V_i} = \mu_0 M_s^2 \frac{V_j}{d_{ij}^3} \cos(\theta_{ij}) \quad (4)$$

where V_i and V_j are the grain volumes and d_{ij} is the distance between their centers. This energy should be compared to W_I which dominates at $H=0$. The ratio between the two energies for two identical grains in contact, having radius a and volume V , is given by:

$$\frac{W_{GG}}{W_I} = \frac{2}{C} \frac{V}{(2a)^3} \frac{\cos(\theta)}{\sin^2(\theta)} \quad (5)$$

where C is a constant of the order of unity. Thus, the contribution of the interactions to the magnetic energy is of the same order of that arising from the easy axis. One can expect that such interactions will reduce the

randomness of the initial magnetization orientations thus suppressing the MR amplitude. We note, however, that if the grains are small, the thermal energy can be strong enough to smear out the interaction effects in a similar manner to the effect on the easy axis as grains become superparamagnetic. Therefore, for smaller grains, the MR amplitude can be larger than that of larger grains. In our mesoscopic samples, in which the average grain size is smaller, the interactions will play a smaller role and the MR magnitude may be larger, as indeed observed in the experiments. This does not depend on the quench condensed sample resistance since the same set of grains dominate the transport throughout the sample growth until the film approaches the metallic phase. In macroscopic samples, adding material increases the average grain size participating in the transport as noted above. The importance of the magnetic interactions (relative to the thermal energy, $k_B T$) thus increases with decreasing resistance. This trend manifests itself in the reduction of $R=R$ with film growth as demonstrated in Fig. 3a.

In summary we point out that reducing the size of any disordered system, so that it enters the mesoscopic regime, is always accompanied by rich phenomena. The case where the sample is ferromagnetic introduces novel effects in addition to the usual sample to sample fluctuations. These include large MR amplitudes, large saturation fields and unique coercivity behavior. We suggest that the experimental findings are indicative of a transition from percolative transport to an effective 1D conductance. In the magnetic case, this enables the detection of the presence of ultra-small grains which are "invisible" in large samples. Assuming magnetic inter-grain correlations enables us to account for the different MR amplitudes measured in macroscopic and mesoscopic samples. Obviously, A more detailed theoretical treatment of the issues discussed in this paper is needed. This is the subject of an ongoing study.

We gratefully acknowledge illuminating discussions with R. Berkovits and technical help from A. Cohen. This research was supported by the Israel Science Foundation (grant number 326/02).

-
- [1] J.I. Gittleman, Y. Goldstein and S. Bozowski, Phys. Rev. B 5, 3609 (1972).
 - [2] A. M. Ilner, A. Geber, B. Groisman, M. Karpovsky and A. G. Laskikh, Phys. Rev. Lett. 76, 475 (1996).
 - [3] W. Yang, Z.S. Jiang, W.N. Wang and Y.W. Du, Solid State Commun. 104, 479 (1997).
 - [4] S. Honda, T. Okada, M. Nawate and M. Tokumoto, Phys. Rev. B 56, 14566 (1997).
 - [5] S. Sankar and A.E. Berkowitz, Appl. Phys. Lett, 73, 535 (1998).
 - [6] A. Frydman and R.C. Dynes, Sol. State Comm., 110,

- 485 (1999).
- [7] A. Frydman, T. L. Kirk and R. C. Dynes, *Solid State Commun.*, 114, 481 (2000).
- [8] J. S. Helman and B. Abeles, *Phys. Rev. Lett.*, 37, 1429 (1976).
- [9] P. Sheng, B. Abeles and Y. Arie, *Phys. Rev. Lett.*, 31, 44 (1973).
- [10] J. C. Slonczewski, *Phys. Rev B* 39, 6995 (1989)
- [11] E. Z. Meilikhov, *JETP* 89, 1184 (1999).
- [12] M. Pollak, *J. Non-crystalline Solids*, 11, 1 (1972).
- [13] V. Ambegaokar, B. I. Halperin and S. Langer, *Phys. Rev. B* 4, 2162 (1971).
- [14] C. J. Adkins, *J. Phys. C: Solid State Phys.*, 15, 7143 (1982).
- [15] A. Miller and E. Abraham, *Phys. Rev.* 120, 745 (1960).
- [16] M. Strongin, R. Thompson, O. Kammerer and J. Crow, *Phys. Rev. B* 1, 1078 (1970).
- [17] R. C. Dynes, J. P. Gamio and J. M. Rowell, *Phys. Rev Lett.* 40, 479 (1978).
- [18] H. M. Jaeger, D. B. Haviland, B. G. Orr, and A. M. Goldman, *Phys. Rev B* 40, 182 (1989).
- [19] R. P. Barber and R. E. Glover, III, *Phys. Rev. B* 42, 6754 (1990).
- [20] A. Frydman and R. C. Dynes, *Phil. Mag.* 81, 1153 (2001).
- [21] A. Cohen, A. Frydman and R. Berkovits, *Solid State Commun.*, 129, 291 (2004).
- [22] H. Vilchik, R. Berkovits and A. Frydman, in preparation.
- [23] R. H. Kodama, A. E. Berkowitz, E. J. McNiff, Jr., and S. Foner, *Phys. Rev. Lett.* 77, 394, (1996).
- [24] The precise value depends on the exact P for Ni which is between 0.23 to 0.47, see R. J. Soulen Jr., J. M. Byers, M. S. Osofsky, B. Nadgorny, T. Ambrose, S. F. Cheng, P. R. Broussard, C. T. Tanaka, J. Nowak, J. S. Moodera, A. Barry and J. M. Coey, *Science*, 282, 85 (1998).